Soft Matter

PAPER

View Article Online
View Journal | View Issue

Cite this: *Soft Matter*, 2019, **15**, 8627

Structure and dynamics of hagfish mucin in different saline environments†

Katerina Rementzi,[ab] Lukas J. Böni,[c] Jozef Adamcik,[c] Peter Fischer*[c] and Dimitris Vlassopoulos*[ab]

The defense mechanism of hagfish against predators is based on its ability to form slime within a few milliseconds. Hagfish slime consists of two main components, namely mucin-like glycoproteins and long protein threads, which together entrap vast amounts of water and thus form a highly dilute hydrogel. Here, we investigate the mucin part of this hydrogel, in particular the role of the saline marine environment on the viscoelasticity and structure. By means of dynamic light scattering (DLS), shear and extensional rheology we probe the diffusion dynamics, the flow behavior, and the longest filament breaking time of hagfish mucin solutions. Using DLS we find a concentration-independent diffusion coefficient – characteristic for polyelectrolytes – up to the entanglement regime of 0.2 mg ml^{-1}, which is about ten times higher than the natural concentration of hagfish mucin in hagfish slime. We also observe a slow relaxation process associated with clustering, probably due to electrostatic interactions. Shear rheology further revealed that hagfish mucin possesses pronounced viscoelastic properties at high concentrations (3 mg ml^{-1}), showing that mucin alone achieves mechanical properties similar to those of natural hagfish slime (mucins and protein threads). The main effects of added seawater salts, and predominantly $CaCl_2$ is to reduce the intensity of the slow relaxation process, which suggests that calcium ions lead to an ionotropic gelation of hagfish mucins.

Received 14th May 2019,
Accepted 11th October 2019

DOI: 10.1039/c9sm00971j

rsc.li/soft-matter-journal

I. Introduction

Marine dwelling hagfishes produce vast amounts of slime when attacked.[1] The slime serves as an immediate defense mechanism against potential predators[2] and acts by clogging their mouth and gills.[3] A glandular white secretion, so-called exudate, is released from the ventrolateral pores of hagfish into the surrounding seawater. The exudate consists of two main components, namely mucin vesicles and protein threads packed into skeins (Fig. 1a). A skein looks like a microscopic 'ball-of-wool' and is made of a single coiled-up protein thread that is up to 30 cm long and 1–3 μm in diameter. When skeins are ejected from the slime glands into the seawater, they unravel and deploy their long intermediate filament bundle fiber, creating a cohesive fiber network of protein threads.[4,5] The other main component, the mucin vesicles contain mucin-like glycoproteins, which are negatively charged by sulphonated side groups.[6–8] Once in contact with seawater, the mucin vesicles swell,

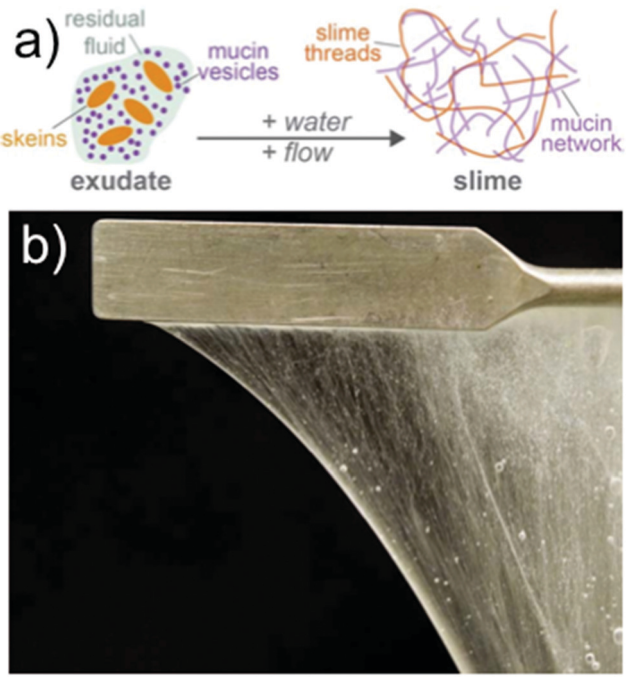

Fig. 1 Illustrations of hagfish slime. (a) Sketch of exudate and hagfish slime formation in water; (b) photo of hagfish slime hanging on a spatula. The cohesivity originates from the long protein threads in hagfish slime.

[a] FORTH, Institute of Electronic Structure & Laser, N. Plastira 100, 70013 Heraklion, Greece. E-mail: dvlasso@iesl.forth.gr
[b] Department of Materials Science & Technology, University of Crete, P.O. Box 2208, 71003 Heraklion, Greece
[c] Institute of Food, Nutrition and Health, ETH Zürich, 8092 Zürich, Switzerland. E-mail: peter.fischer@hest.ethz.ch

† Electronic supplementary information (ESI) available. See DOI: 10.1039/c9sm00971j

rupture, and discharge their mucin.[9] The hydrated mucin and the network of unraveled skeins synergistically form hagfish slime (Fig. 1b). Hagfish slime is in many ways an exceptional natural hydrogel. It can physically confine up to 26 000 times its own weight in water given its sieve-like structure made by the protein threads and mucin. Also, it forms within milliseconds in high osmolarity seawater, is coherent, elastic yet extremely soft,[10,11] which is a unique combination of features for hydrogels found in nature.

The fact that a charged gel with a complex network structure rapidly deploys in a strongly charge-screening environment as in seawater (ionic strength of about 0.7 M[12]) is intriguing and has led to studies that investigated the effects of ionic strength and ionic composition. The main areas of focus comprised the effects of salts on *ex vivo* stabilization of hagfish exudate,[8,13–15] skein unraveling,[16,17] mucin vesicle swelling and rupture,[9,16–18] swelling and hydration of skeins[19] and reconstituted biomimetic materials made from slime thread proteins,[20] and whole hagfish slime functionality.[17] These studies show (i) that a high osmolarity of about 800 mOsmol l^{-1} and higher achieved by divalent anions (sulfate, citrate, phosphate) stabilizes hagfish exudate,[8,14,15] (ii) that seawater assists the dissolution of a glue, which holds the native skeins together and mediates unraveling,[16] (iii) that protein threads and materials made from those protein swell less in high osmolarity environments,[19,20] (iv) that viscosities of mucin solutions are lower in seawater than in deionized water,[11,17] and (v) that swelling and rupture of hagfish mucin vesicles requires the presence calcium ions when the ionic strength of the solution is >100 mM.[18] Especially calcium ions seem to exert critical roles in hagfish slime functionality.[17] First, calcium ions are considered to keep the polyanionic mucin molecules within the vesicles in a condensed state before swelling.[9,21] Second, Ca^{2+}–ions were shown to be important for mucin vesicle decondensation by activating Ca^{2+}-mediated transporter proteins in the vesicle membrane, which facilitate water influx and swelling of mucin vesicles.[18] And third, Ca^{2+}–ions were found to be crucial in realizing a functional slime network. Calcium seems to be required for an ionotropic gelation of hagfish mucin, forming a non-covalently stabilized mucin network inside the slime that retains the water.[17] Ionotropic gelation, also called polyelectrolyte complexation is based on the ability of polyelectrolyte molecules to form hydrogels in the presence of counterions even below the entanglement concentration.[22–25]

Although previous works studied hagfish mucin vesicles and hagfish mucin in stabilization solutions and different saline environments, still little is known about the fundamental interactions of hagfish mucin with salts and especially calcium ions. In this work we investigated the structure and dynamics of hagfish mucin over broad length and time domains and focused especially on the effect of different salt environments. Using atomic force microscopy, we first elucidate the size and morphology of single mucin vesicles and mucin molecules. Advanced light scattering and extensional rheology were then used to explore the diffusion and disentanglement kinematics of hagfish mucin over a broad range of concentrations and thus determine an entanglement concentration, which was found to be much higher than the natural concentration of hagfish mucin. In a last part, we investigate the effect of calcium ions on the intra- and intermolecular diffusion of mucin molecules and show how they affect the rheological properties.

II. Materials & methods

Sample collection

Sample collection was conducted according to a protocol described by Böni *et al.*[13] In brief, Atlantic hagfish (*Myxine glutinosa*) were kindly fished in the Fjords of Ålesund by the staff of the Atlanterhavsparken (Norway). A mixture of 1 : 9 of clove bud oil (Sigma-Aldrich) and ethanol was used for hagfish anesthetization. Sedated hagfish were placed on a dissection board and plotted dry. Subsequently, electrical stimulation (HPG1, Velleman Instruments, 80 Hz, 8–18 V) was used on the ventrolateral side of the sedated hagfish to contract the local muscles and thus expel the exudate from the slime pores. A polished spatula was used to remove the secreted exudate, which was immediately stabilized in a high osmolarity citrate-PIPES (CP) buffer consisting of 0.9 M sodium citrate and 0.1 M PIPES at pH 6.7, 0.02% NaN_3 and a protease inhibitor. Samples were stored at 4 °C. After sampling hagfish were allowed to recover and subsequently release back to the sea. Sampling procedure was performed in accordance with the approved ethical application by the Forsøksdyrutvalget (FOTS ID 6912).

Sample preparation

The vesicle stock suspension was prepared according to the protocol of Salo *et al.*[8] In brief, exudate stabilized in high osmolarity buffer was filtered through a series (60 and 20 μm) of nylon mesh filters (Merck) to separate the small mucin vesicles from the skeins. To obtain a high mucin vesicle concentration, the filtrate was centrifuged at 2000 g for 10 minutes and the supernatant discarded. The mucin content of the vesicle suspension was determined in triplicates by dialysis (25 kDa MWCO, Spectra-Por, USA), *i.e.* dialyzing 0.5 ml of the vesicle suspension against three batches of Milli-Q water (12 h each) and subsequent freeze drying to determine the dry weight. Hagfish mucin solutions were prepared by mixing stabilized mucin vesicles with Milli-Q water or solutions containing the salts of interest in a 2 ml Eppendorf tube, sloshing it heads over eight times. Mucin solutions containing maximum 1% of the vesicle stock suspension were prepared. If lower percentages of vesicle stock suspensions were used, the final mucin solution was adjusted for ionic strength by adding the required amount of CP buffer to achieve 1% CP buffer in the solution. Artificial seawater (ASW) was prepared according to a recipe of Kester *et al.*[12] All salts were obtained from Sigma. For the dissolved salts a complete dissociation was assumed.

Microscopy

Atomic force microscopy (AFM) for vesicle imaging was performed on a Cypher (Asylum Research, USA) and on a Bruker FastScan microscope (Bruker, USA) for mucin imaging. Images were acquired in tapping mode in air and water, using BioLevers Mini (Olympus, Japan) to image the vesicles and

RTESPA 150 cantilevers (Bruker, USA) for the mucin. To prepare the vesicle sample, a droplet of vesicles in CP buffer was put on a silicon wafer and let to rest for about three hours so the vesicles could sink and weakly stick to the surface. For the mucin, repeatedly washed vesicles stock suspension was dialyzed (25 kDa MWCO, SpectraPor, USA) Milli-Q (three batches, 12 h each). The dialyzed samples were filled into 15 ml Falcon tubes and diluted with Milli-Q to get a mucin concentration of roughly 0.2 mg ml^{-1}. Droplet of mucin solution (mucin dialysed against Milli-Q or see water) was deposited on freshly cleaved mica, adsorbed for 2 min, washed with Milli-Q water and dried by air. Cryo-Scanning electron microscopy (cryo-SEM) was performed on a LEO 1530 (Carl-Zeiss SMT AG). Vesicles in CP buffer were snap frozen with a high-pressure freezer (Bal-Tec HPM100), freeze-fractured (Bal-Tec BAF060), sputter coated (SCD 050 sputter coater, Bal-Tec) with a 3 nm thick platinum layer and then imaged.

Dynamic light scattering

Dynamic light scattering (DLS) measurements were carried out using a ALV-5000 system (ALV, Germany) operating with a polarized monochromatic laser beam at a wavelength of λ = 532 nm. The temperature was controlled using a recirculating fluid bath (15 °C < T < 50 °C). The scattered intensity was detected by the photomultiplier and analyzed in a correlator yielding eventually information about the relaxation dynamics of the measured object. The scattering angles between incident and scattered light ($25^\circ < \theta < 150^\circ$) define the scattering wavevector $q = (4\pi n/\lambda)\sin(\theta/2)$, which is the inverse length scale probed (0.00681 nm^{-1} < q < 0.03039 nm^{-1}), where n is the refractive index. The intensity correlation function is expressed as:

$$g^{(2)}(\tau) = \frac{\langle I(t)I(t+\tau)\rangle}{\langle I(t)\rangle} \quad (1)$$

through the Siegert relation:

$$g^{(2)}(\tau) = B + \beta|g^{(1)}|^2 \quad (2)$$

where B represents the baseline and β the coherent factor, $g^{(1)}$ is the electric field correlation function and τ is the delay time.[26,27] The analysis of the data after the computational Laplace transform yield the distribution of decay rate $G(\Gamma)$ and defined as:

$$g^{(1)}(\tau) = \int G(\Gamma)\exp(-\Gamma\tau)\mathrm{d}\Gamma \quad (3)$$

where $G(\Gamma)$ is the normalized distribution of decay rates, the quantity related directly to the diffusion is the decay rate $\Gamma = D_{\mathrm{app}}q^2$ where D_{app} is the diffusion coefficient of the scattering particles into the suspension. Considering a spherical particle the diffusion coefficient is given by the Stokes–Einstein–Sutherland equation:[28]

$$D_{\mathrm{app}} = \frac{k_{\mathrm{B}}T}{6\pi\eta R} \quad (4)$$

where k_{B} is the Boltzmann constant, η is the viscosity of the solvent and R is the hydrodynamic radius of the particles. The correlation functions were analyzed with the non-linear cumulant analysis (NLCA). The following equation explained as a more robust procedure as well explained from Mailer *et al.*[29] The non-linear fit is:

$$g^{(2)} = B + \beta\left\{\exp(\bar{\Gamma}\tau)\left[1 + \frac{1}{2}\mu_2\tau^2 - \frac{1}{3!}\mu_3\tau^3 + \frac{1}{4!}\mu_4\tau^2 - \cdots\right]\right\}^2 \quad (5)$$

where the baseline B is 1 for ideal conditions and μ_2, μ_3,... represent the order of cumulants with μ_2 being the second cumulant.

Shear and extensional rheology

Oscillatory shear and creep measurements were conducted with a MCR501 rheometer from Anton-Paar (Austria) using a cone-plate geometry with a diameter of 50 mm and a cone angle of 1° (truncation of 102 μm). Measurements were performed at 20 °C. For extensional rheometry the CaBER 1 rheometer (Thermo Haake, Thermo Fisher Scientific) was used. Cylindrical plates with diameter of 6 mm were used. An initial gap of 3 mm and a final gap of 12 mm were chosen, using a strike time of t_{s} = 50 ms. The sample was loaded with a micropipette (80 μL) on the bottom plate, an initial step strain was applied and as a result a liquid filament was formed. Within this capillary an extensional flow field establishes. For Newtonian liquids the capillary diameter decreases linearly with time. For viscoelastic fluids such as polymer solutions large non-Newtonian elastic stresses can grow during the transient elongational stretching process. If these elastic stresses start to dominate during capillary thinning and the corresponding viscous stresses become negligible, an elasto-capillary force balance predicts that the radius of the filament decays exponentially in time:[30]

$$\frac{d_{\mathrm{mid}}(\tau)}{d_{\mathrm{o}}} \approx \left(\frac{G_{\mathrm{app}}d_{\mathrm{o}}}{4\sigma}\right)^{\frac{1}{s}}\exp\left[-\frac{\tau}{3\lambda}\right] \quad (6)$$

where d_0 is the diameter of the bottom and the upper plate, G_{app} is an apparent elastic modulus, σ is the surface tension, λ is the longest relaxation time and s a fitting parameter set to 3. The relaxation time is a time scale associated with the decrease of filament diameter and the apparent elastic modulus reflects the elasticity of the measured fluid during the elasto-capillary thinning. By fitting eqn (6) to the diameter profile, one can obtain the relaxation time and the apparent elastic modulus. The measurements were conducted at room temperature.

III. Results

Vesicle and mucin structure

Fig. 2a shows an atomic force microscopy (AFM) image of a mucin vesicle taken in citrate-PIPES (CP) buffer. The inlet depicts the height profile of the vesicle along the longest axis. An isolated vesicle has an oval-like shape and resembles a disk (3.5 μm long and 200–400 nm high) and shows tiny bumps on its surface, of which the origin and function are yet unknown. The oval disk shape and the bumps are also confirmed in cryo-SEM images (Fig. 2b). Additional cryo-Sem images can be found in Fig. S1 (ESI†).

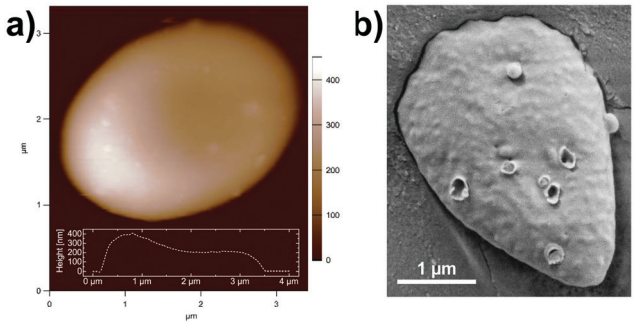

Fig. 2 (a) AFM image taken in CP buffer solution and (b) cryo-SEM image of a hagfish mucin vesicle stabilized in CP buffer solution.

When in contact with water, mucin vesicles swell and release the mucin macromolecules. Fig. 3a displays AFM images of native mucin forming long bundled fibrillar structures. Fig. 3b and c show AFM image of the individual chains of mucin dialyzed in Milli-Q and sea water revealing the different morphology under different ionic conditions.

Dynamics and rheology of mucin at different concentrations

Dynamic light scattering (DLS) measurements probe the internal dynamics of hagfish mucin. As shown by AFM images above, hagfish mucins are very large filamentous macromolecules with lengths L of the order of micrometers, resulting in $qR > 1$. The analysis of the intermediate scattering (time autocorrelation) functions of mucin solutions at various concentrations resulted in a very large observed size at $q = 0.01204$ nm^{-1} (Fig. 4a), which is assigned to the hydrodynamic correlation length ξ_H (mesh size of the network). Under the present conditions the investigated samples are ergodic as confirmed by the large (and only weakly changing) total amplitude of the intermediate scattering functions and the fact that slow modes relax within the experimental time window. The highest concentration of 3.47 g ml^{-1} may be at the onset of non-ergodicity but the fast relaxation dynamics, which is of concern in this work, is virtually unaffected. This is typical situation in weak gels, which have been studied with conventional, time-averaged DLS.[26,27,31] The non-ergodic regime is beyond the scope requires spartical averaging of the intermediate scattering function.[27,32] In Fig. 4b the apparent diffusion coefficient for a mucin concentration of $c_{mucin} = 0.08$ mg ml^{-1} is shown. From the measurement the

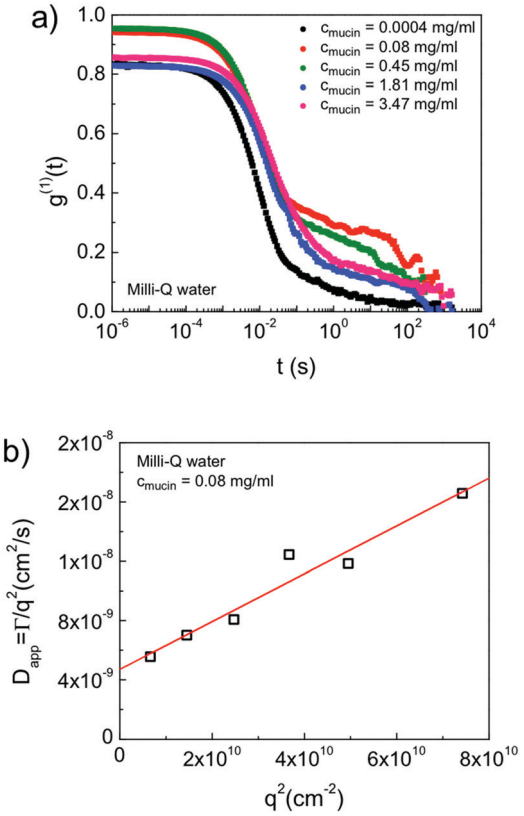

Fig. 4 DLS on the dynamics of hagfish mucin in Milli-Q water. (a) Intermediate scattering functions ($C(q, t) = g^{(2)} - 1$) at different mucin concentrations in water at $\theta = 45°$ ($q = 0.01204$ nm^{-1}). (b) Extracted apparent diffusion coefficient $D_{app}(q \to 0)$ for $c_{mucin} = 0.08$ mg ml^{-1} (line to guide the eye, representative errors are summarized in Fig. 5).

apparent diffusion coefficient $D_{app}(q \to 0) = 4.7 \times 10^{-9}$ cm^{-2} s^{-1} and a respective hydrodynamic correlation length $\xi_H = 455$ nm were extracted. Apparent diffusion coefficients for a wider range of mucin concentrations (4.3×10^{-4}–3.47 mg ml^{-1}) showed a similar trend as in Fig. 4b and are summarized in Fig. S2 (ESI†). Furthermore, the scattering intensity for all mucin concentrations depends strongly and virtually identically on the scattering wavevector q (Fig. S3, ESI†), pointing to large length scales with the internal structure of mucin being independent of concentration.[33]

In Fig. 5 the apparent diffusion coefficient as a function of mucin concentration is summarized. Starting from a concentration

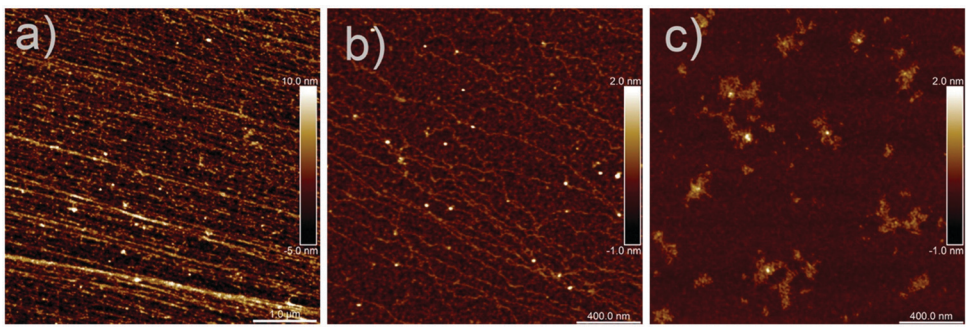

Fig. 3 AFM image of (a) native mucin, (b) mucin dialyzed in Milli-Q water and (c) mucin dialyzed in seawater.

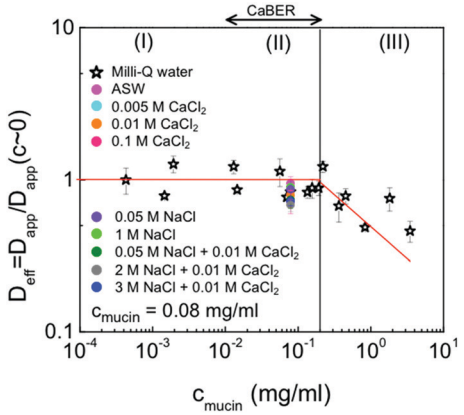

Fig. 5 Effective diffusion coefficient as a function of mucin concentration and salts added to the mucin solution. Regime (I) is the dilute, regime (II) the semidilute, and regime (III) the entanglement region. The double arrow indicates the CaBER working regime and the vertical line indicates the transition from the semidilute to the entanglement regime ($c_{mucin} > 0.2$ mg ml^{-1}). Different colors for $c_{mucin} = 0.08$ mg ml^{-1} represent the extracted diffusion coefficient in the presence of salts in the mucin solution.

of 0.2 mg ml^{-1} the diffusion coefficients start to decline. This indicates that the mucin entanglement concentration in Milli-Q is around 0.2 mg ml^{-1}. Fig. 5 also shows that the addition of various salts added to the mucin solution does not substantially affect the diffusion coefficient at the reference concentration of 0.08 mg ml^{-1}. The low q region at $q \rightarrow 0$ is not detectable and in order to estimate the $I(q)$ we used the Debye plot (Fig. S4, ESI†) and the reduced total intensity (Fig. S5, ESI†). The intensity remains constant until it reaches the concentration of 0.2 mg ml^{-1}, which is in a good agreement with the diffusion coefficient against the same range of concentrations.

At high mucin concentrations ($c_{mucin} = 3$ mg ml^{-1}), oscillatory shear data (Fig. 6a) suggest a viscoelastic mucin network, which shows a predominant elastic modulus G' and weakly frequency dependent moduli, *i.e.* indicating a typical soft gel-like behavior. To access the low-frequency crossover of the viscoelastic moduli, a step stress creep test at shear stress of $\sigma = 0.04$ Pa was applied for 21 h and reveals a stress relaxation process of hagfish mucin at the crossover frequency of $\omega = 10^{-5}$ rad s^{-1} or a stress relaxation time of about 20 hours. In Fig. 6b capillary breakup extensional rheometry (CaBER) measurements are shown. The normalized diameter of the formed capillaries decays as function of time for four mucin concentrations. The curves show a pronounced elasto-capillary breakup regime, supporting the viscoelastic behavior observed in oscillatory shear flow, also at lower concentrations. From the elasto-capillary breakup, an extensional relaxation time λ and the apparent modulus G_{app} can be extracted, which are plotted together with the filament break-up time t_B in Fig. 6c. The apparent modulus G_{app} in extension is consistent with the storage modulus G' measured in shear.

Effects of sea water salts on hagfish mucin

The effect of salts and salt concentration on hagfish mucin was studied using artificial seawater (ASW). Typical intermediate scattering (time autocorrelation) functions for mucin solutions

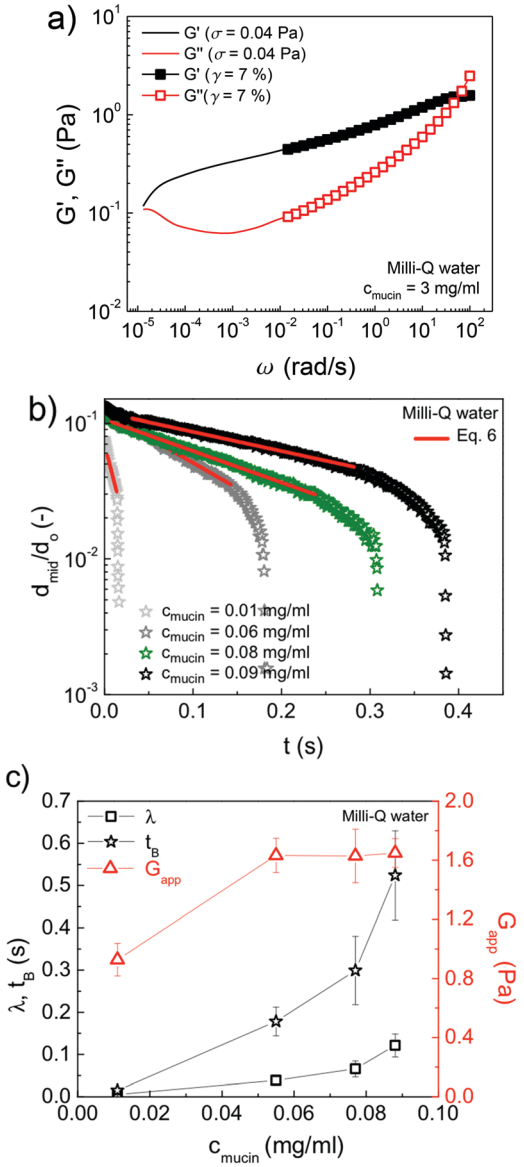

Fig. 6 Shear and extensional rheology of hagfish mucin in Milli-Q water. (a) Storage and loss moduli (G' and G'') as a function of frequency ω in the linear viscoelastic regime at 20 °C for a mucin concentration of 3 mg ml^{-1}. (b) CaBER measurements showing the filament diameter over time normalized with the diameter of the plate for various mucins concentration. (c) Extensional relaxation time λ, break-up time t_B, and apparent modulus G_{app} as functions of mucin concentration (error bars are calculated from ten individual measurements).

in ASW are depicted in Fig. 7a where a dominant fast relaxation process (10^{-3} s $< t <$ 10^{-1} s) is observed, along with a slow relaxation process (10^{-1} s $< t <$ 10^{1} s). The investigated samples are ergodic as in the context of Fig. 4a. The analysis of the fast relaxation process reveals an apparent diffusion coefficient of $D_{app}(q \rightarrow 0) = 5.32 \times 10^{-9}$ cm^2 s^{-1} (Fig. 7b). Fig. 7c shows the filament thinning CaBER experiment of mucin in dilutions of ASW. With increasing ASW concentrations, the capillary lifetime reduces. This suggests that in the absence of seawater salts hagfish mucin possesses a higher viscoelasticity, which

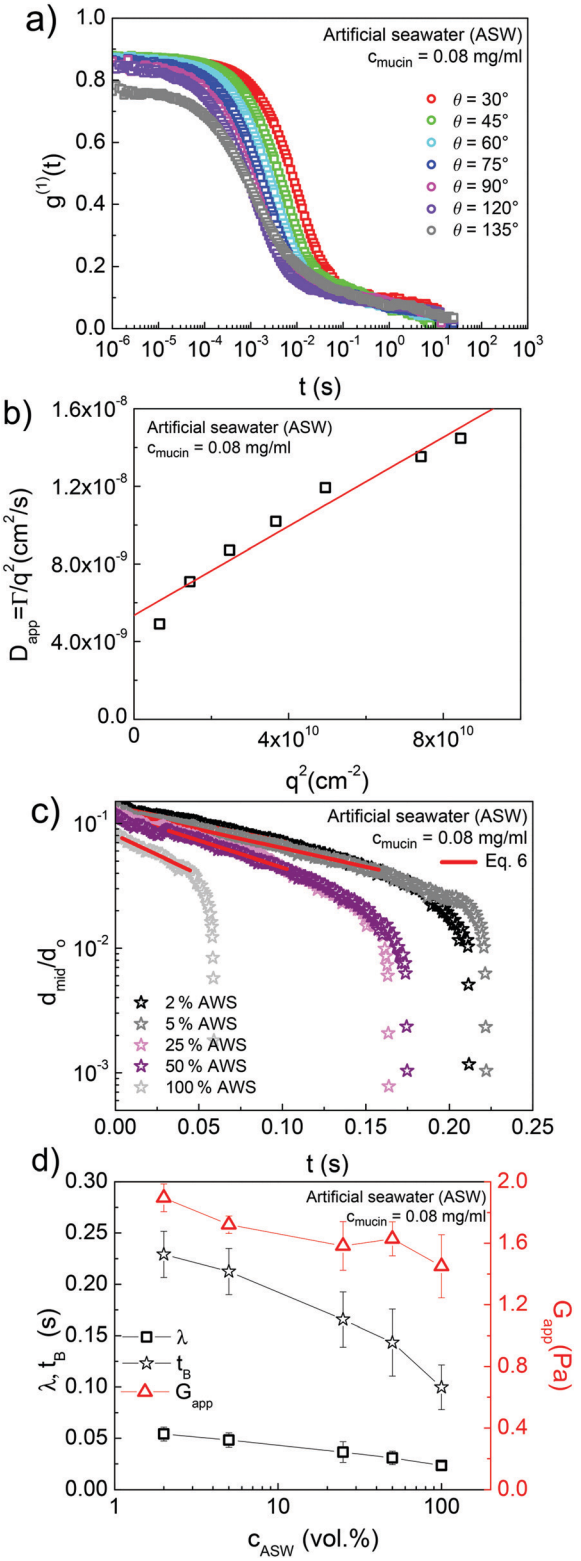

Fig. 7 DLS measurements and extensional rheology of hagfish mucin at different dilution of artificial seawater (ASW) (a) Intermediate scattering functions ($C(q,t) = g^{(2)} - 1$) of mucins at a concentration c_{mucin} = 0.08 mg ml^{-1}. (b) Extraction of the apparent diffusion coefficient for c_{mucin} = 0.08 mg ml^{-1}. (c) CaBER measurements showing the diameter of the filament normalized with the diameter of the plate at various dilutions of ASW. (d) Extensional relaxation time λ, break-up time t_B, and apparent modulus G_{app} as a function of ASW concentration (error bars are calculated from ten individual measurements).

was similarly shown for the viscosity of hagfish mucin.[11,17] The corresponding extensional relaxation time λ, break-up time t_B, and the apparent modulus G_{app} are depicted in Fig. 7d. All extracted parameters decrease with an increase in ASW concentration.

Effects of seawater ions and in particular $CaCl_2$

The effect of Ca^{2+} was investigated with respect to possible calcium-mediated ionic bridges and their implications on the dynamic properties of mucin. Fig. 8a depicts the measured (ergodic, see above) intermediate scattering functions of mucin solutions without and with added calcium at increasing concentrations: 0.005, 0.01 (natural), and 0.1 M of $CaCl_2$. Measurements in saline environments showed a more pronounced slow mode. The evidence for Ca^{2+}–ion bonds is also shown in Fig. 8b at $q > 0.02225$ nm^{-1} by the decrease in the apparent diffusion coefficient for salt-free samples and samples with 0.1 M of $CaCl_2$. The decrease of the diffusion coefficient is generally observed for all added salts as depicted in Fig. 8b (large q-values as indicated by the arrow) and suggests a network formation of mucins. In the absence of salt (empty triangles) the apparent

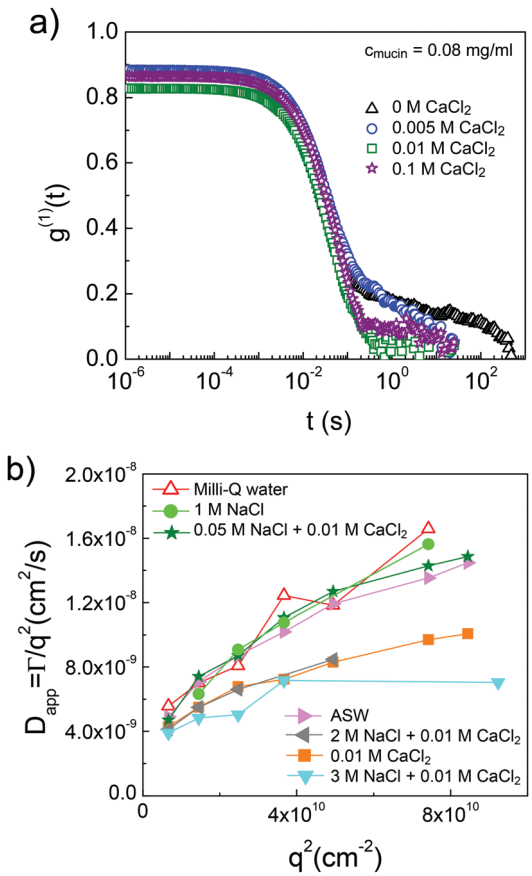

Fig. 8 DLS on the dynamics of hagfish mucins in saline environments. (a) Intermediate scattering functions of mucin at a concentration c_{mucin} = 0.08 mg ml^{-1} in salt-free environment and at various concentrations of $CaCl_2$: 0.005, 0.01, and 0.1 M (θ = 30°, *i.e.* q = 0.00814 nm^{-1}). (b) Apparent diffusion coefficient for a mucin concentration of c_{mucin} = 0.08 mg ml^{-1} in different saline environments.

diffusion coefficient D_{app} has the highest values and drops with the addition of salts. The highest reduction is seen for a mixture of 3 M of NaCl and 0.01 M $CaCl_2$ (blue triangle). The DLS measurements were performed at very long-time intervals (4500 s) for the salt-free samples while measurements in saline environments were performed at long-time intervals as well as in cumulated 20 time intervals of 100 s (Fig. S6–S8, ESI†) for a mucin solution with 0.1 M $CaCl_2$. The cumulated measurements were performed to obtain good statistics and extract reliable information about the main (fast) relaxation process (Fig. S7 and S8, ESI†) while the slow mode (long relaxation time) is captured in the long-time interval measurement.

Mucin network formation by calcium is further supported by extensional rheology (Fig. 9). CaBER measurements show that both, the extensional relaxation time λ and break-up times t_B follow the same trend: both values rise (Region I) until a peak is observed at the natural calcium concentration of 0.01 M. Above this concentration, both times constants rapidly decrease and reach a plateau (Region II). In Region I vesicles open up mediated by calcium and release mucin[18,19] until the natural concentration of 0.01 M $CaCl_2$ is reached. Beyond the natural calcium concentration, we speculate that the network collapses because of the attractive interactions, which dominate within mucin molecules (Ca^{2+} bridges).

IV. Discussion

Vesicle and mucin structure

In this study the structure and dynamics of hagfish mucin were investigated. A particular focus was put on the effect of mucin concentration and ionic composition of the surrounding liquid. As shown in Fig. 2, mucin vesicles are disk-shaped with sizes in the range of roughly 0.4 μm (height) to 2 μm (width) to 3–4 μm (length). The vesicles open up in contact with water and release mucin macromolecules, which form hagfish mucus – the part of hagfish slime without protein threads. AFM images revealed that hagfish mucins are in the micrometers length-scale, which agrees well with the large size reported for other mucins. However, unlike human or pig mucin glycoproteins, hagfish mucins did not show the typically observed "ball-and-chain structure".[34,35] Their different molecular composition – 80% protein and 20% sugar residues in contrast to other mucins that are 20% protein and 80% sugar residues[8] – could be a possible explanation for the absence of the ball-and-chain structure.

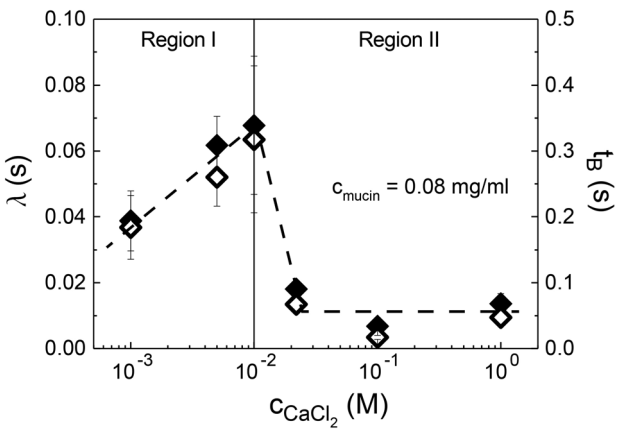

Fig. 9 Extensional relaxation time λ and break-up time t_B of mucin at a concentration c_{mucin} = 0.08 mg ml^{-1} plotted against $CaCl_2$ concentration. Two regimes are observed, increasing time constants at low concentrations (Region I), which are followed by a peak (peak at c_{CaCl_2} = 0.01 M) and a decrease at larger $CaCl_2$ concentrations in Region II (error bars are calculated from ten individual measurements, dashed line to guide the eye).

Mucin concentration dependence

The presence of large molecules with substantial polydispersity was further implied by the occurrence of a slow relaxation process in the DLS measurements under various environmental conditions (Fig. 4a, 7a and 8a). Due to their large size, the apparent diffusion coefficient depends on the scattering wavevector (Fig. 4b), which is observed for all measured mucin concentrations (Fig. S2, ESI†). The intensity profiles $I(q)$ scale with q^{-3}, highlighting the presence of a wide spanning network. Based on this result, the internal dynamics of the system are probed. The apparent static correlation length ξ of about ~100 nm is smaller than the hydrodynamic correlation length ξ_H (~ 400 nm) extracted from the apparent diffusion coefficient (Fig. S9, ESI†). However, both ξ_H and ξ are nearly insensitive to mucin and salt concentrations (Fig. S10, ESI†). The small but albeit unambiguous difference between these two length scales is not surprising for such large objects: it reflects the measurement of a highly heterogeneous mucin network (see Fig. 3) and the associated statistical analysis of the probed signal.[36] The assignment of these length scales to the mesh size of the formed mucin network is supported by the AFM image of mucin solution in Fig. 3. It shows a heterogeneous network with long filaments which are entangled and the mesh size is polydisperse but of the order of 100 nm. By increasing the mucin concentration (Fig. S9, ESI†), we note that (i) the internal structure remains similar, (ii) the characteristic size (ξ and ξ_H) is unchanged and (iii) the moduli extracted from extensional rheology (*i.e.* G_{app}) are almost independent of concentration. This evidence suggests that as the concentration increases the network structure (mesh size and associated modulus) does not change, but instead the length of the filaments increases. This is a likely scenario as single mucin molecules are known to dimerize and subsequently polymerize *via* disulfide bond formation.[35,37,38] This behavior suggests self-similarity for hagfish mucins, which was already postulated for whole hagfish slime by Chaudhary *et al.*[33]

DLS measurements for mucins in Milli-Q water further showed that the diffusion coefficient is constant at lower mucin concentrations but decreases at a mucin concentration of about c_{mucin} = 0.2 mg ml^{-1}. In Fig. 5, three distinct regions highlight the dilute (I), the semidilute (II), and the entanglement regime (III). For non-charged polymers the dilute and the semidilute regime are well distinguished by the overlapping of macromolecules leading to a slowdown of the diffusion coefficient. In charged systems such as polyelectrolytes and thus also for hagfish mucin, ions prevent the overlap and

penetration of macromolecules. Their ion-impaired configuration gives rise to a constant diffusion coefficient in an extended concentration regime (regime I and II in Fig. 5).[39] For hagfish mucin, the apparent diffusion coefficient remains constant for three decades in concentration before decreasing at c_{mucin} = 0.2 mg ml^{-1}. The entanglement concentration of 0.2 mg ml^{-1} is about ten times higher than the natural concentration and thus ten time less economic for the hagfish to rely as defense system.[11] Polymeric systems operating below their entanglement concentration generally do not show pronounced and characteristic macroscopic flow features, which however is the case with hagfish slime. This raises the question, if together with the protein thread network the mucin could start to show its characteristic rheological behavior below the entanglement concentration by using the thread network as anchor points and thus similarly reach an entanglement concentration, as already suggested by us before.[40]

Rheological signature of the mucin network

The shear rheological properties of hagfish mucin is shown in Fig. 6a. At a mucin concentration of c_{mucin} = 3 mg ml^{-1} a plateau for the storage modulus G' and a minimum of the loss modulus G'' is observed, which is the signature of a physical network and can be attributed to entangled or interacting mucin molecules. The mucin solution exhibits terminal flow after roughly 21 hours, suggesting that it is highly viscoelastic albeit with low plateau modulus. The latter value is in a good agreement with those reported for other mucin systems.[41] This is the first time that the viscoelastic network of hagfish mucin was measured in shear rheology, *i.e.* in the absence of the protein threads. It is considered that in natural hagfish slime the protein threads dominate the rheological signal, mainly contributing to the observed viscoelasticity ($G' \sim 0.02$ Pa at natural conditions of mucins and protein threads).[10,33] However, in absence of protein threads and at mucin concentrations higher than naturally employed, the elastic modulus G' can exceed 0.5 Pa (Fig. 6a) resulting in networks strengths 100 times higher that of natural hagfish slime including the protein threads. These results suggest that the mucin component also contribute to the viscoelasticity in natural hagfish slime and supports the idea that protein threads act as anchor points in natural hagfish slime.[35] In Fig. 6b the capillary thinning of hagfish mucin at different concentrations in Milli-Q water is shown. The increase of mucin concentration slows down the capillary thinning process and leads to a longer elasto-capillary thinning regime. Relaxation times extracted from the CaBER measurements increased with mucin concentration (Fig. 6c). At higher concentrated mucin solutions (*e.g.* above c_{mucin} = 0.1 mg ml^{-1}) slower filament thinning and eventually no break-up but beads-on-a-string formation is observed (data not shown). Extensional and shear rheology yield similar values of the viscoelastic moduli.

The role of ions present in artificial seawater (ASW)

The presence of salts, both monovalent (NaCl, KCl, *etc.*) and divalent ($CaCl_2$, $MgCl_2$, *etc.*) increase the electrostatic screening within mucins due to the high ionic strength environment. Since the natural environment corresponds to 100% seawater, ions affect both the apparent diffusion coefficient and the rheological response of the mucin. In Fig. 7a, the similar shape of the $I(q)$ curves including the presence of slow modes are attributed to the homogenous ion distribution. From the apparent diffusion coefficient, we extract the hydrodynamic radius R_H of 400 nm, which is similar to the size in the salt-free environment (Milli-Q water). By increasing the concentration of seawater, the initial thinning dynamics in CaBER experiments were accelerated due to the high ionic strength of the ASW (Fig. 7c). Consequently, the relaxation time λ, the apparent elastic modulus G_{app}, and the break-up time t_B showed a reduction when the concentration of seawater was increased (Fig. 7d), which was similarly shown for the dynamic viscosity of hagfish mucin.[17] In extensional rheology, we propose that the electrostatic screening hinders a coil-to-stretch transition of the mucin polyelectrolytes under flow and therefore causes shorter relaxation times and break-up times with increasing ASW concentration. Coil-stretch transitions are well known in dilute solutions of linear high-molecular-weight polymers in extensional flows. If strain rates are above a critical value, polymers unravel from a loose spherical shape to an extended state, causing a spectacular increase in extensional resistance.[42,43] Two conditions must be satisfied in order for polymers to be stretched: first, the strain rate must be large enough to stretch the polymer, meaning the strain rate must exceed the relaxation rate ($1/\lambda$) of the molecule. And second, the strain rate must be applied for a sufficient time for the polymer molecule to accumulate the strain.[44,45] For hagfish slime defense, reduced relaxation and break-up times in ASW compared to dilutions of ASW would mean less defensive potential as the loss in slime viscoelasticity was suggested to prevent efficient gill clogging with would-be predators.[40] Above 0.003 M $CaCl_2$ (*i.e.* 30% ASW) all vesicles open due to calcium mediated vesicle swelling[18] whereas below 0.1 M NaCl also all vesicles open due to hypo-osmolarity.[17] With all dilutions of ASW all vesicles should always be open – triggered by calcium or hypo-osmolarity and thus the observed effect is unlikely to be caused by mucin concentration but rather by electrostatic screening effects.

The particular role of calcium ions

Herr *et al.*[18] showed that Ca^{2+}–ions are important for mucin vesicle decondensation by activating Ca^{2+}-mediated transporter proteins in the vesicle membrane, which facilitate water influx and swelling of mucin vesicles. The authors showed that in seawater strength osmolarity a calcium concentration of 0.003 M is sufficient to trigger the opening of all mucin vesicles. Although calcium promotes the opening of the vesicles, concentrations exceeding 0.01 M (being the natural concentration in the sea) dramatically weakened the extensional response as can be seen by the nearly vanishing relaxation times (Fig. 9, Region II). These measurements suggest a structural collapse of the mucin molecules, which is also reflected in the DLS signals (Fig. 8) because they exhibit pronounced slow modes.

The reduced extensional signal and occurrence of slow modes in DLS measurements strongly support the suggestion that calcium causes an ionotropic gelation, as mucins knowingly form reversible network formation and create salt-bridges between their chains with calcium.[46–48]

V. Conclusions

Hagfish slime consists of two main components, mucin-like glycoproteins and protein threads initially coiled up in skeins, which together form a highly dilute hydrogel. Their synergistic interplay in high ionic strength seawater allows for a sophisticated and properly working defense system. We investigated the dynamics and structure of the mucin hydrogel in the presence and absence of seawater ions. Once in contact with water the hagfish mucin vesicles swell and release their mucin macromolecules. AFM imaging revealed the nano-morphology of the mucin vesicles, showing their disk like oval shape and a rough surface, which was confirmed with electron microscopy. Furthermore, the structure and size of single mucin molecules could be shown, revealing their large size (15–50 μm) and providing a mesh size. Using DLS, also the hydrodynamic radius ($R_H \sim 400$ nm) of the mucin macromolecules was obtained for both Milli-Q and ionic environment. The scattering intensity for all mucin concentrations scaled with the scattering wave vector q with a power-law slope of – 3, suggesting that the internal structure of mucin is independent of concentration and therefore possesses self-similar features. The emerging picture calls for a heterogeneous network whose structure is virtually unchanged with increasing concentration while concomitantly its constituting filaments increase in length by means of self-assembly. The entanglement concentration of hagfish mucin was found to be 0.2 mg ml^{-1}. This concentration is one order of magnitude higher than the natural amount of mucin in hagfish slime (0.02 mg ml^{-1}). Small oscillatory shear rheology revealed pronounced viscoelastic properties at high concentrations (3 mg ml^{-1}), showing that mucin alone achieved mechanical properties similar to those of natural hagfish slime (mucins and protein threads). As the current opinion is that the mucin part in hagfish slime does not contribute to viscoelasticity, this finding implies that viscoelasticity of the natural slime may not exclusively be governed by the protein threads. The presence of seawater ions did not alter significantly the hydrodynamic radius R_H compared to Milli-Q water. However, the thinning dynamics in extensional rheometry experiments were accelerated and consequently the relaxation time λ, the apparent elastic modulus G_{app}, and the break-up time t_B were reduced due to the high ionic strength of the ASW. It is likely that electrostatic screening hinders a coil-to-stretch transition of the mucin in the extensional flow. Calcium ions were found to strongly mediate viscoelasticity at concentrations below the natural calcium concentration in seawater (0.01 M). Calcium concentrations higher than 0.01 M lead to a collapse of structure of the mucin gel, which was manifested by the loss of the ability to form capillaries in extensional rheology as well as the occurrence of pronounced slow modes in DLS measurement. The observed slow mode in the intensity ($I(q)$ curves) indicate a reduced dynamic of the topologically constrained mucin molecules, most likely caused by their polyelectrolyte character and their interaction with calcium ions. The reduced extensional signal and occurrence of slow modes in DLS measurements strongly support the suggestion that calcium leads to an ionotropic gelation of hagfish mucin. Future work, especially at higher mucin concentrations and mucus formulations will help further exploring the properties of this fascinating class of materials. In this respect, the eventual non-ergodicity and the possible emergence of surface layers during measurements are important challenges to address.

Conflicts of interest

There are no conflicts to declare.

Acknowledgements

LJB and PF acknowledge funding from ETH Zürich (Grant ETH-1914-1).

References

1 T. J. Parker and W. A. Haswell, *A textbook of zoology*, Macmillan, 1910.
2 V. Zintzen, C. D. Roberts, M. J. Anderson, A. L. Stewart, C. D. Struthers and E. S. Harvey, Hagfish predatory behaviour and slime defence mechanism, *Sci. Rep.*, 2011, **1**, 131.
3 J. Lim, D. S. Fudge, N. Levy and J. M. Gosline, Hagfish slime ecomechanics: testing the gill-clogging hypothesis, *J. Exp. Biol.*, 2006, **209**, 702–710.
4 S. W. Downing, R. H. Spitzer, W. L. Salo, J. S. Downing, L. J. Saidel and E. A. Koch, Threads in the hagfish slime gland thread cells: organization, biochemical features, and length, *Science*, 1981, **212**, 326–328.
5 B. Fernholm, Thread Cells from the Slime Glands of Hagfish (Myxinidae), *Acta Zool.*, 1981, **62**, 137–145.
6 L. Böcker, P. A. Rühs, L. Böni, P. Fischer and S. Kuster, Fiber-Enforced Hydrogels: Hagfish Slime Stabilized with Biopolymers including κ-Carrageenan, *ACS Biomater. Sci. Eng.*, 2016, **2**, 90–95.
7 L. Böni, P. A. Rühs, E. J. Windhab, P. Fischer and S. Kuster, Gelation of Soy Milk with Hagfish Exudate Creates a Flocculated and Fibrous Emulsion- and Particle Gel, *PLoS One*, 2016, **11**, e0147022.
8 W. L. Salo, S. W. Downing, W. A. Lidinsky, W. H. Gallagher, R. H. Spitzer and E. A. Koch, Fractionation of hagfish slime gland secretions: partial characterization of the mucous vesicle fraction, *Prep. Biochem.*, 1983, **13**, 103–135.
9 J. E. Herr, T. M. Winegard, M. J. O'Donnell, P. H. Yancey and D. S. Fudge, Stabilization and swelling of hagfish slime mucin vesicles, *J. Exp. Biol.*, 2010, **213**, 1092–1099.

10 R. H. Ewoldt, T. M. Winegard and D. S. Fudge, Non-linear viscoelasticity of hagfish slime, *Int. J. Non Linear Mech.*, 2011, **46**, 627–636.
11 D. S. Fudge, N. Levy, S. Chiu and J. M. Gosline, Composition, morphology and mechanics of hagfish slime, *J. Exp. Biol.*, 2005, **208**, 4613–4625.
12 D. R. Kester, I. W. Duedall, D. N. Connors and R. M. Pytkowicz, Preparation Of Artificial Seawater, *Limnol. Oceanogr.*, 1967, **12**, 176–179.
13 L. J. Böni, R. Zurflüh, M. Widmer, P. Fischer, E. J. Windhab, P. A. Rühs and S. Kuster, Hagfish slime exudate stabilization and its effect on slime formation and functionality, *Biol. Open*, 2017, **6**, 1115–1122.
14 S. W. Downing, W. L. Salo, R. H. Spitzer and E. A. Koch, The hagfish slime gland: a model system for studying the biology of mucus, *Science*, 1981, **214**, 1143–1145.
15 D. L. Luchtel, A. W. Martin and I. Deyrup-Olsen, Ultrastructure and permeability characteristics of the membranes of mucous granules of the hagfish, *Tissue Cell*, 1991, **23**, 939–948.
16 M. A. Bernards Jr., I. Oke, A. Heyland and D. S. Fudge, Spontaneous unraveling of hagfish slime thread skeins is mediated by a seawater-soluble protein adhesive, *J. Exp. Biol.*, 2014, **217**, 1263–1268.
17 L. J. Böni, R. Zurflüh, M. E. Baumgartner, E. J. Windhab, P. Fischer, S. Kuster and P. A. Rühs, Effect of ionic strength and seawater cations on hagfish slime formation, *Sci. Rep.*, 2018, **8**, 9867.
18 J. E. Herr, A. M. Clifford, G. G. Goss and D. S. Fudge, Defensive slime formation in Pacific hagfish requires Ca2 – and aquaporin-mediated swelling of released mucin vesicles, *J. Exp. Biol.*, 2014, **217**, 2288–2296.
19 M. A. Bernards Jr., S. Schorno, E. McKenzie, T. M. Winegard, I. Oke, D. Plachetzki and D. S. Fudge, Unraveling interspecies differences in hagfish slime skein deployment, *J. Exp. Biol.*, 2018, **221**, jeb176925.
20 L. J. Böni, A. Sanchez-Ferrer, M. Widmer, M. D. Biviano, R. Mezzenga, E. J. Windhab, R. R. Dagastine and P. Fischer, Structure and Nanomechanics of Dry and Hydrated Intermediate Filament Films and Fibers Produced from Hagfish Slime Fibers, *ACS Appl. Mater. Interfaces*, 2018, **10**, 40460–40473.
21 P. Verdugo, I. Deyrup-Olsen, M. Aitken, M. Villalon and D. Johnson, Molecular mechanism of mucin secretion: I. The role of intragranular charge shielding, *J. Dent. Res.*, 1987, **66**, 506–508.
22 S. H. Ching, N. Bansal and B. Bhandari, Alginate gel particles–A review of production techniques and physical properties, *Crit. Rev. Food Sci. Nutr.*, 2017, **57**, 1133–1152.
23 H. Kleine-Brueggeney, G. K. Zorzi, T. Fecker, N. E. El Gueddari, B. M. Moerschbacher and F. M. Goycoolea, A rational approach towards the design of chitosan-based nanoparticles obtained by ionotropic gelation, *Colloids Surf., B*, 2015, **135**, 99–108.
24 M. A. Patel, M. H. H. AbouGhaly, J. V. Schryer-Praga and K. Chadwick, The effect of ionotropic gelation residence time on alginate cross-linking and properties, *Carbohydr. Polym.*, 2017, **155**, 362–371.
25 V. Pillay, C. M. Dangor, T. Govender, K. R. Moopanar and N. Hurbans, Ionotropic gelation: Encapsulation of indomethacin in calcium alginate gel discs, *J. Microencapsulation*, 1998, **15**, 215–226.
26 J. Marakis, K. Wunderlich, M. Klapper, D. Vlassopoulos, G. Fytas and K. Müllen, Strong Physical Hydrogels from Fibrillar Supramolecular Assemblies of Poly(ethylene glycol) Functionalized Hexaphenylbenzenes, *Macromolecules*, 2016, **49**, 3516–3525.
27 M. Shibayama, Y. Fujikawa and S. Nomura, Dynamic Light Scattering Study of Poly(*N*-isopropylacrylamide-*co*-acrylic acid) Gels, *Macromolecules*, 1996, **29**, 6535–6540.
28 D. K. Carpenter, Dynamic Light Scattering with Applications to Chemistry, Biology, and Physics (Berne, Bruce J.; Pecora, Robert), *J. Chem. Educ.*, 1977, **54**, A430.
29 A. G. Mailer, P. S. Clegg and P. N. Pusey, Particle sizing by dynamic light scattering: non-linear cumulant analysis, *J. Phys.: Condens. Matter*, 2015, **27**, 145102.
30 S. L. Anna and G. H. McKinley, Elasto-capillary thinning and breakup of model elastic l iquids, *J. Rheol.*, 2001, **45**, 115–138.
31 M. Gianneli, R. F. Roskamp, U. Jonas, B. Loppinet, G. Fytas and W. Knoll, Dynamics of swollen gel layers anchored to solid surfaces, *Soft Matter*, 2008, **4**, 1443–1447.
32 A.-M. Philippe, L. Cipelletti and D. Larobina, Mucus as an Arrested Phase Separation Gel, *Macromolecules*, 2017, **50**, 8221–8230.
33 G. Chaudhary, D. S. Fudge, B. Macias-Rodriguez and R. H. Ewoldt, Concentration-independent mechanics and structure of hagfish slime, *Acta Biomater.*, 2018, **79**, 123–134.
34 R. Bansil, E. Stanley and J. T. Lamont, Mucin Biophysics, *Annu. Rev. Physiol.*, 1995, **57**, 635–657.
35 R. Bansil and B. S. Turner, Mucin structure, aggregation, physiological functions and biomedical applications, *Curr. Opin. Colloid Interface Sci.*, 2006, **11**, 164–170.
36 A. Aggeli, G. Fytas, D. Vlassopoulos, T. C. McLeish, P. J. Mawer and N. Boden, Structure and dynamics of self-assembling beta-sheet peptide tapes by dynamic light scattering, *Biomacromolecules*, 2001, **2**, 378–388.
37 R. Bansil, J. P. Celli, J. M. Hardcastle and B. S. Turner, The Influence of Mucus Microstructure and Rheology in Helicobacter pylori Infection, *Front. Immunol.*, 2013, **4**, 310.
38 J. K. Sheehan, S. Kirkham, M. Howard, P. Woodman, S. Kutay, C. Brazeau, J. Buckley and D. J. Thornton, Identification of molecular intermediates in the assembly pathway of the MUC5AC mucin, *J. Biol. Chem.*, 2004, **279**, 15698–15705.
39 R. H. Colby, Structure and linear viscoelasticity of flexible polymer solutions: comparison of polyelectrolyte and neutral polymer solutions, *Rheol. Acta*, 2010, **49**, 425–442.
40 L. Böni, P. Fischer, L. Böcker, S. Kuster and P. A. Rühs, Hagfish slime and mucin flow properties and their implications for defense, *Sci. Rep.*, 2016, **6**, 30371.
41 S. K. Lai, Y.-Y. Wang, D. Wirtz and J. Hanes, Micro- and macrorheology of mucus, *Adv. Drug Delivery Rev.*, 2009, **61**, 86–100.

42 P. P. Bhat, S. Appathurai, M. T. Harris, M. Pasquali, G. H. McKinley and O. A. Basaran, Formation of beads-on-a-string structures during break-up of viscoelastic filaments, *Nat. Phys.*, 2010, **6**, 625–631.

43 R. G. Larson and J. J. Magda, Coil-stretch transitions in mixed shear and extensional flows of dilute polymer solutions, *Macromolecules*, 1989, **22**, 3004–3010.

44 P. G. D. Gennes and P. G. De Gennes, Coil-stretch transition of dilute flexible polymers under ultrahigh velocity gradients, *J. Chem. Phys.*, 1974, **60**, 5030–5042.

45 E. J. Hinch, Mechanical models of dilute polymer solutions in strong flows, *Phys. Fluids*, 1977, **20**, S22.

46 J. F. Forstner and G. G. Forstner, Calcium binding to intestinal goblet cell mucin, *Biochim. Biophys. Acta*, 1975, **386**, 283–292.

47 B. D. E. Raynal, T. E. Hardingham, J. K. Sheehan and D. J. Thornton, Calcium-dependent protein interactions in MUC5B provide reversible cross-links in salivary mucus, *J. Biol. Chem.*, 2003, **278**, 28703–28710.

48 C. Ridley, N. Kouvatsos, B. D. Raynal, M. Howard, R. F. Collins, J.-L. Desseyn, T. A. Jowitt, C. Baldock, C. W. Davis, T. E. Hardingham and D. J. Thornton, Assembly of the respiratory mucin MUC5B: a new model for a gel-forming mucin, *J. Biol. Chem.*, 2014, **289**, 16409–16420.